LAMINAR FULLY DEVELOPED MIXED CONVECTION WITH VISCOUS DISSIPATION IN A UNIFORMLY HEATED VERTICAL DOUBLE-PASSAGE CHANNEL

by

Mostafa M. Salah El-Din

Fully developed laminar mixed convection has been investigated numerically in a vertical double-passage channel by taking into account the effect of viscous dissipation. The channel is divided into two passages by means of a thin, perfectly conductive plane baffle and the walls are uniformly heated. The effects of Brinkman number and the ratio between Grashof and Reynolds numbers on the velocity and temperature profiles and the Nusselt number on the hot wall have been analyzed. The results show that these effects depend mainly on the baffle position.

Key words: *convection, channel, double-passage, uniform heat flux*

Introduction

Enhancement of the heat transfer in a vertical channel is a major aim because of its practical importance in many engineering systems, such as the solar energy collection [1, 2] and the cooling of electronic systems [3, 4]. The convective heat transfer may be enhanced in a vertical channel by using rough surface, inserts, swirl flow device, turbulent promoter, *etc*. [5]. Candra *et al*. [6, 7] investigated the use of ribbed walls, Han *et al*. [8] used V-shaped turbulence promoters, Lin *et al*. [9] and Beitelmal *et al*. [10] demonstrated the effect of jet impingement mechanism. Recently, Dutta and Hossain [11] investigated the heat transfer and the frictional loss in a rectangular channel with inclined solid and perforated baffles.

Unfortunately, most of these methods cause a considerable drop in the pressure. Guo *et al*. [12] suggested that the convective heat transfer could be enhanced by using special inserts, which can be specially designed to increase the included angle between the velocity vector and the temperature gradient vector rather than to promote turbulence. So, the heat transfer is considerably enhanced with as little pressure drop as possible. A plane baffle may be used as an insert to enhance the rate of heat transfer in the channel. To avoid a considerable increase in the transverse thermal resistance into the channel, a thin and perfectly conductive baffle is used. The effect of such baffle on the heat transfer in a vertical channel can be found elsewhere [13, 14].

In a previous work [15], the effect of viscous dissipation on fully developed laminar mixed convection in a vertical double-passage channel with uniform wall temperatures has been investigated numerically. Although viscous dissipation is usually neglected in low-speed and low-viscosity flows through conventionally sized channels of short lengths, it may become important when the length-to-width ratio is large [16]. As an illustration, the working dimensions are: length = 1.2 m, width = 0.2 m and the volume flow rate = 1 10^{-5} m^3/s [17]. For double–passage channels, the length-to-width ratio becomes larger as the baffle becomes near the wall. So, viscous dissipation may become important.

For the fully developed laminar duct flow, Guo *et al.* [12] observed that Nu for the case of the isoflux thermal boundary condition is greater than Nu for the case of isothermal boundary condition. This can be explained based on the concept of the included angle between the velocity and temperature gradient vectors. This angle is larger at isoflux thermal boundary condition than at isothermal boundary condition. Therefore, they stated that changing the thermal boundary condition could enhance the convective heat transfer. Fully developed flow is closely approached in a channel whose length is large compared with its width. The study of this flow is, therefore, useful; it is also instructive because it yields the limiting conditions for the developing flow. Aung *et al.* [18] have found that when L 10^{-2} (L = Gr l/b, l is the length) the case is fully developed. Therefore, the present work is devoted to study, numerically, the effect of viscous dissipation on fully developed mixed convection in a vertical double-passage channel with uniform wall heat flux.

Analysis

The channel shown in fig. 1 is divided into two passages by means of a perfectly conductive and thin baffle. Laminar, two-dimensional, incompressible, steady flow is considered. The fluid properties are assumed to be constant except for the buoyancy term of the momentum equation. The channel walls have uniform heat fluxes.

For fully developed flow, it is assumed that the transverse velocity is zero and the pressure depends only on x. The governing equations, expressing the above conditions, are:

$$v\frac{\mathrm{d}^2 u_i}{\mathrm{d}y^2} \quad \mathrm{g}\beta(T \quad T_0) \quad \frac{1}{\rho_0}\frac{\mathrm{d}p_i}{\mathrm{d}x} \tag{1}$$

$$k\frac{\partial^2 T}{\partial y^2} \quad \mu\left(\frac{\mathrm{d}u}{\mathrm{d}y}\right)^2 \quad \rho_0 c_{\mathrm{p}} u\frac{\partial T}{\partial x} \tag{2}$$

The subscript "*i*" denotes stream 1 or stream 2.

It should be noted that many authors [13, 19, 20] used the entering fluid temperature as a reference temperature. This allows comparison with the numerical solution of

the developing flow problem at great distances from the entry, but is rather bizarre as far as the fully developed flow is concerned. The momentum balance eq. (1) has been written according to the Boussinesq approximation by invoking a linearization of the equation of state $\rho(T)$ around the reference temperature T_0. Barletta and Zanchini [21] recommended the choice of the mean fluid temperature as the reference temperature in the fully developed region. This choice ensures that at each channel section, the average square deviation from the local temperature is minimum and, as a consequence, yields the best conditions for the validity of the equation of state $\rho(T)$. Recently, Boulama and Galanis [22] adopted the temperature of the cooler wall as reference, because it leads to simple expressions for the thermal boundary conditions. In particular, the value of the

Figure 1. Physical configuration of the double-passage channel

dimensionless temperature at this wall equals zero. In the present work, the choice of Barletta and Zanchini is used. So the reference temperature is defined as:
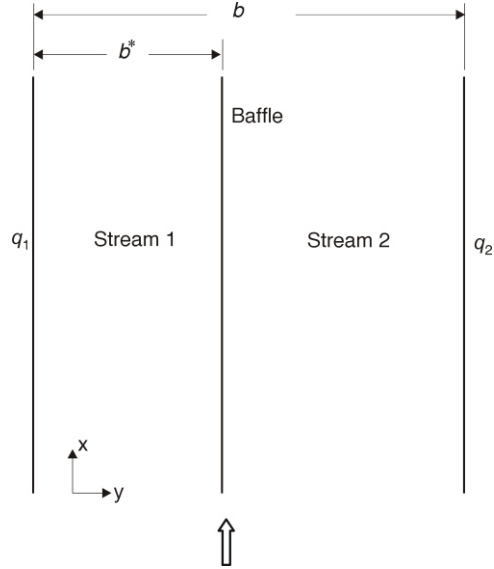
$$T_0 = \frac{1}{b} \int_0^b T \, dy \qquad (3)$$

The boundary conditions are:

$$y = 0: \quad u_1 = 0, \quad \frac{\partial T}{\partial y} = -\frac{q_1}{k}$$

$$y = b^*: \quad u_1 = u_2 = 0, \quad T_1 = T_2$$

$$y = b: \quad u_2 = 0, \quad \frac{\partial T}{\partial y} = \frac{q_2}{k}$$

Integration of eq. (2) with respect to y yields:

$$k \frac{\partial T}{\partial y}\bigg|_{y=b} - k \frac{\partial T}{\partial y}\bigg|_{y=0} + \mu \int_0^b \left(\frac{du}{dy}\right)^2 dy = \rho_0 c_p \frac{\partial T}{\partial x} \int_0^b u \, dy \qquad (4)$$

The first two terms of LHS of eq. (4) represent the heat fluxes on the walls and the integration in RHS represents the mass flow rate within the channel, which is constant at any cross-section. The reference velocity u_0 is defined as:

$$u_0 = \frac{1}{b} \int_0^b u\, dy \tag{5}$$

Thus, eq. (4) can be rewritten as:

$$\frac{\partial T}{\partial x} = \frac{1}{\rho_0 c_p b u_0} \left[q_1 + q_2 + \mu \int_0^b \left(\frac{du}{dy} \right)^2 dy \right] \tag{6}$$

Now, the energy equation can be rewritten as:

$$k \frac{\partial^2 T}{\partial y^2} + \mu \left(\frac{du}{dy} \right)^2 = \frac{u}{u_0 b} \left[q_1 + q_2 + \mu \int_0^b \left(\frac{du}{dy} \right)^2 dy \right] \tag{7}$$

To make the governing equations dimensionless, the following dimensionless quantities are introduced:

$$X = \frac{x}{b\mathrm{Re}}, \quad Y = \frac{y}{b}, \quad U = \frac{u}{u_0}$$

$$\theta = \frac{T - T_0}{\frac{q_1 b}{k}}, \quad \mathrm{Gr} = \frac{g\beta q_1 b^4}{v^2 k}, \quad R = \frac{q_2}{q_1}$$

$$P = \frac{p}{\rho_0 u_0^2}, \quad \mathrm{Re} = \frac{u_0 b}{v}, \quad \mathrm{Br} = \frac{\mu u_0^2}{q_1 b}$$

Hence, the dimensionless governing equations are:

$$\frac{d^2 U_i}{dY^2} = \frac{\mathrm{Gr}}{\mathrm{Re}}\theta_i + \frac{dP_i}{dX} \tag{8}$$

$$\frac{\partial^2 \theta}{\partial Y^2} + \mathrm{Br} \left(\frac{dU}{dY} \right)^2 = \left[1 + R + \mathrm{Br} \int_0^1 \left(\frac{dU}{dY} \right)^2 dY \right] U = \eta U \tag{9}$$

where

$$\eta = 1 + R + \mathrm{Br} \int_0^1 \left(\frac{dU}{dY} \right)^2 dY \tag{10}$$

The pressure gradient in eq. (8) is assumed to be constant, *i. e.*:

$$\frac{dP_i}{dX} \quad \gamma_i \tag{11}$$

Introduction of the dimensionless parameters into eq. (3) gives:

$$\int_0^1 \theta dY \quad 0 \tag{12}$$

The dimensionless boundary conditions are:

$$Y \quad 0: \; U_1 \quad 0, \; \frac{\partial \theta}{\partial Y} \quad 1$$
$$Y \quad Y^*: \; U_1 \quad U_2 \quad 0, \; \theta_1 \quad \theta_2$$
$$Y \quad 1: \; U_2 \quad 0, \; \frac{\partial \theta}{\partial Y} \quad R$$

where

$$Y^* \quad \frac{b^*}{b}$$

Conservation of mass considered at any section of the channel passages gives:

$$\int_0^{Y^*} U_1 dY \quad Y^* \tag{13}$$

and

$$\int_{Y^*}^1 U_2 dY \quad 1 \quad Y^* \tag{14}$$

The dimensionless bulk temperature in passage 1 is:

$$\theta_{bl} \quad \frac{\displaystyle\int_0^{Y^*} U_1 \theta dY}{\displaystyle\int_0^{Y^*} U_1 dY} \quad \frac{\displaystyle\int_0^{Y^*} U_1 \theta dY}{Y^*} \tag{15}$$

The Nusselt number on the hot wall is:

$$Nu_1 \quad \frac{1}{\theta|_{Y \; 0} \quad \theta_{bl}} \tag{16}$$

Numerical methodology

Investigation of the governing equations formulated shows that the energy equation and the momentum equation are coupled and non-linear. Furthermore, for uniform wall heat fluxes the wall's temperatures are not specified. Therefore, the solutions can be

obtained by use of an iterative scheme with successive approximations. The equations are first approximated by finite difference equations. Then, the following solution procedure is used:

(1) guess the walls' temperatures,
(2) guess a temperature field at the interior points inside the whole channel,
(3) solve the momentum equation, using eqs. (13) and (14), to obtain the velocity field and the pressure gradient for the two streams separately,
(4) solve the energy equation, using eq. (12) and the values of the velocity of the previous step, to obtain new values of the temperature at the interior points inside the whole channel and the value of η,
(5) by means of a three-point derivative formula, using the temperature values computed at step 4, compute new values for the wall's temperatures, and
(6) return to step 3 and repeat until convergence.

A uniform grid in the Y-direction is used with equal numbers of grid points for each passage (41 points). Thus, a smaller grid size in the narrower passage will be obtained. The solution procedure and grid sizes were validated by comparison with the case when the effect of viscous dissipation is neglected. For this case eq. (10) gives:

$$\eta \quad 1 \quad R \tag{17}$$

The numerical results of η against the values from eq. (17) are shown in tab. 1 for different values of R. It is found that the deviations in η are always less than 1.4%.

Table 1. Calculations of η without viscous dissipation (Gr/Re = 100, Br = 0, Y* = 0.5)

R	1	0.5	0
η (eq. 17)	2	1.5	1
η (numerical)	1.97217	1.496515	0.9977519

Furthermore, the calculations were carried out for the flow without buoyancy forces. For this case the analytical solution of the momentum equation gives:

$$\gamma_1 \quad 12/Y^{*2} \quad \text{and} \quad \gamma_2 \quad 12/(1 \quad Y^*)^2 \tag{18}$$

The numerical calculations give very close values to those calculated using eq. (18). For example, at $Y^* = 0.5$ eq. (18) gives $\gamma_1 = \gamma_2 = -48$ while the numerical calculations give $\gamma_1 = \gamma_2 = -47.99993$. This confirms the accuracy and convergence of the numerical calculations.

Results and discussions

The governing equations formulated with the given boundary conditions show that the numerical calculations depend on the following parameters: R, Br, Y^*, and Gr/Re.
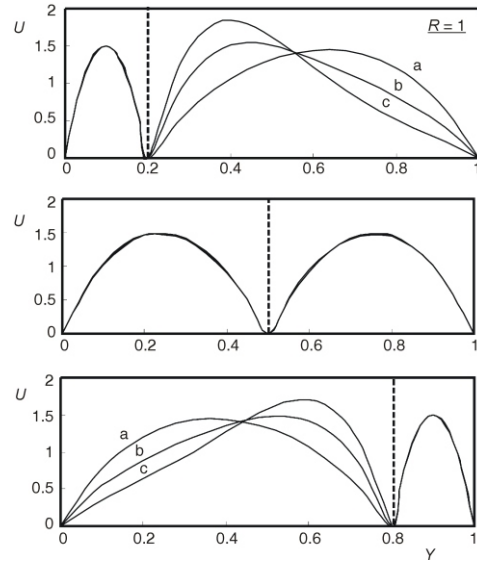
When the parameter Gr/Re exceeds a threshold value, flow reversal may occur causing downflow along the cooler wall. Since the equations are parabolic in their nature, unstable solutions are expected when the flow reversal occurs. Examination of the flow reversal phenomenon is beyond the scope of this study. Therefore, the solution procedure was immediately stopped when a negative velocity has been attained. For more discussions of the flow reversal phenomenon see Aung and Worku [19, 23].

In the following sections the effect of Br and Gr/Re on the Nu on the hot wall will be presented at different positions of the baffle with symmetric heating ($R = 1$), asymmetric heating ($R = 0.5$), and one wall is adiabatic ($R = 0$). The chosen values for Br and Gr/Re are commonly found in the application of cooling of electronic systems. First, the velocity and temperature profiles will be presented because of their usefulness in clarification of the heat transfer mechanism in the channel.
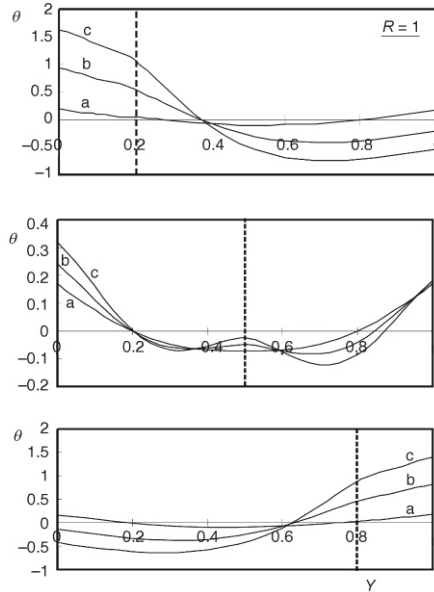

Figure 2. Effect of Br on velocity profiles for symmetric heating
(a) Br = 0, (b) Br = 0.05, (c) Br = 0.1
(Gr/Re = 100)

The effect of Br on the velocity profiles for symmetric heating is shown in fig. 2 at different positions of the baffle. The figure reveals that the effect of Br appears clearly in the wider passage, while in the narrower passage its effect is not noticeable. When the baffle is in the middle of the channel very slight effects of viscous dissipation can be noticed in both passages. The maximum velocity point moves towards the baffle as Br increases.

The energy equation shows that the temperature profile depends on the velocity profile. Since the velocity profiles depend on the baffle position, it is expected that the temperature profiles depend on the baffle position too. Figure 3 presents the effect of Br on the temperature profiles for the case of symmetric heating at different positions of the baffle. The figure reveals that an increase in Br increases the temperature significantly in the narrower passage. This is due to the increasing in viscous heating since the length-to-width ratio is large in the narrower passage. This increasing in temperature in the narrower passage is accompanied with a significant decrease in temperature next to the wall of the wider passage. This can be explained with the aid of eq. (12) which implies that the integration of the temperature through the whole channel is zero.

Indeed the increase in Br increases the temperature and hence the velocity increases due to the increase in thermal buoyancy force, but at the same time the increase in Br increases the pressure gradient, which decreases the velocity. For narrower passage, in

Figure 3. Effect of Br on velocity profiles for symmetric heating
(a) Br = 0, (b) Br = 0.05, (c) Br = 0.1
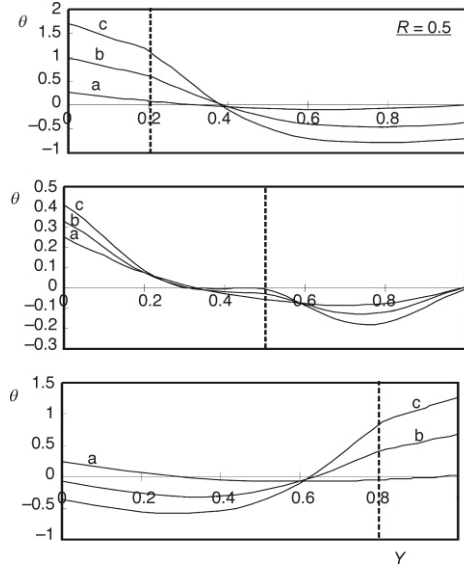*(Gr/Re = = 100)*

which the length-to-width ratio is large, the increase in the pressure gradient is high enough to resist the increase in thermal buoyancy force. So, Br has insignificant effect on the velocity profile. For the wider passage, the high increase in the temperature near the baffle makes the thermal buoyancy force the dominant force. Hence, the velocity increases with Br near the baffle. Consequently, the velocity decreases with Br near the wall, since the mass flow is constant at any cross-section of the channel passages.

The effect of Br on the velocity profiles for $R = 0.5$ and 0 are similar to that for the case of symmetric heating except that a slight decrease in velocity is noticed near the cool wall when the heat flux ratio becomes smaller. This is due to the decrease in the buoyancy forces there. The effects of Br on the temperature profiles at different positions of the baffle for the cases of asymmetric heating and one wall is adiabatic are shown in figs. 4 and 5, respectively. For Br = 0, the temperature on the hot wall is greater than that on the cool wall. For Br > 0, the effect of viscous dissipation on the temperature profiles is similar to that for the case of symmetric heating.

Table 2 and fig. 6 present the variations of Nu_1 with Br at different positions of the baffle for symmetric heating. The table shows that for $Y^* = 0.5$, Nu_1 is a decreasing function of Br. This can be explained with the aid of fig. 3 which shows that for $Y^* = 0.5$, $\theta|_{Y=0}$ is an increasing function of Br. So, the denominator of eq. (16) increases and as a consequence, Nu_1 decreases. Table 2 shows also that the rate of decreasing in Nu_1, due to the increasing in Br, increases as the baffle is nearer to wall 1. As mentioned before, this is because of the increasing of the effect of viscous dissipation as the length-to-width ratio becomes large. It may be noted that at a given value of Br, Nu_1 increases as the baffle is nearer to wall 1. This is due to the increase in the included angle between the velocity vector and the temperature gradient vector.

When the baffle is nearer to wall 2, Nu_1 increases up to a very high value as Br increases. With more increasing in Br, Nu_1 changes its sign. Figure 3 shows that the dimensionless temperature on the wall from which the baffle is far is a decreasing function of Br. So, the difference between the wall temperature and the bulk temperature in the denominator of eq. (16) becomes very small and as a consequence, the value of Nu_1 becomes very high. More increasing in Br makes the denominator of eq. (16) negative and as a consequence, Nu_1 changes its sign.

Figure 4. Effect of Br on temperature profiles for asymmetric heating
(a) Br = 0, (b) Br = 0.05, (c) Br = 0.1 (Gr/Re = 100)
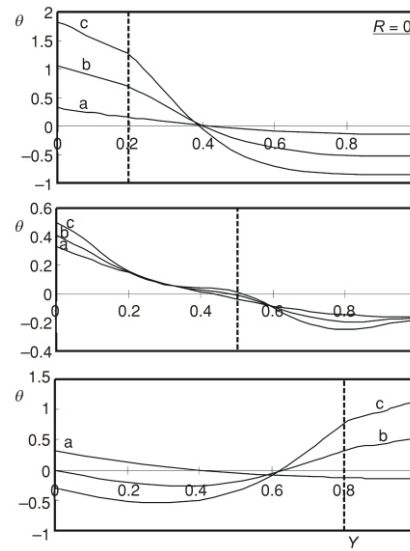
Figure 5. Effect of Br on temperature profiles with an adiabatic wall
(a) Br = 0, (b) Br = 0.05, (c) Br = 0.1 (Gr/Re = 100)

Table 2. Variations of Nu_1 with Br at defferent positions of the baffle for symmetric heting ($R = 1$, Gr/Re = 100)

Br 10^2	Nu_1		
	$Y^* = 0.2$	$Y^* = 0.5$	$Y^* = 0.8$
0	11.51	5.63	4.57
1	9.58	5.24	5.18
2	8.18	4.95	6.12
3	7.29	4.67	7.49
4	6.7	4.43	11.1
5	6.26	4.2	19.11
6	5.8	4	78.6
7	5.35	3.8	−35.6
8	4.98	3.62	−14.7
9	4.65	3.46	−8.75
10	4.37	3.29	−6.11

The variations of Nu_1 with Br are presented in tab. 3 and fig. 7 for asymmetric heating ($R = 0.5$) at different positions of the baffle. From the table it is evident that Nu_1 varies with Br in a manner similar to that for the case of symmetric heating except that the change in sign of Nu_1 at $Y^* = 0.8$ occurs at higher value of Br than that for symmetric heating. As mentioned before, this is due to that the heat flux on the hot wall is greater than that on the cool wall. With an adiabatic wall ($R = 0$) more viscous heating is required to change the sign of Nu_1 at $Y^* = 0.8$ as shown in tab. 4 and fig. 8. To show the effect of the baffle on heat transfer in the channel, it is useful to know the value of Nu_1 for a single-passage channel. From a previous work [24] Nu_1 1 for Br = 0.
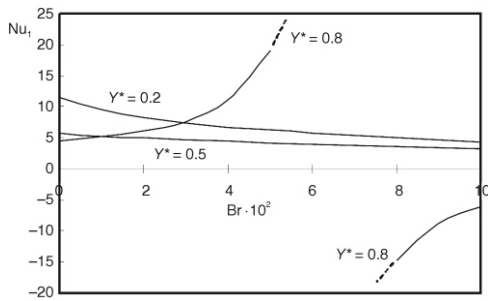

Figure 6. Variations of Nu_1 with Br at different positions of the baffle for symmetric heating ($R = 1$, Gr/Re = 100)
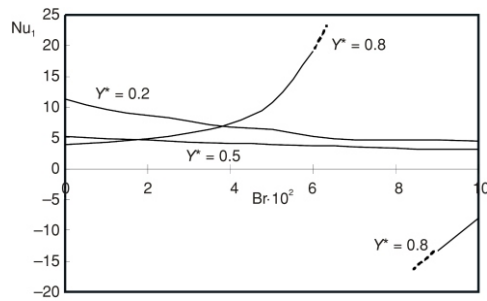
Figure 7. Variations of Nu_1 with Br at different positions of the baffle for asymmetric heating ($R = 0.5$, Gr/Re = 100)

Table 3. Variations of Nu_1 with Br at different positions of the baffle for asymmetric heating ($R = 0.5$, Gr/Re = 100)

Br 10^2	$Y^* = 0.2$	Nu_1 $Y^* = 0.5$	$Y^* = 0.8$
0	11.36	5.16	3.97
1	9.64	4.87	4.36
2	8.58	4.6	4.96
3	7.79	4.36	5.9
4	6.83	4.14	7.25
5	6.37	3.93	10.82
6	5.29	3.74	19.1
7	4.77	3.56	93.23
8	4.72	3.4	−31.53
9	4.69	3.25	−13.33
10	4.4	3.1	−7.97

Table 4. Variations of Nu$_1$ with Br at different positions of the baffle with an adiabatic wall (R = 0, Gr/Re = 100)

Br 10^2	Y^* = 0.2	Nu$_1$ Y^* = 0.5	Y^* = 0.8
0	11.75	4.83	3.54
1	10.21	4.55	3.79
2	8.87	4.32	4.17
3	7.86	4.09	4.76
4	7.05	3.9	5.76
5	6.41	3.72	7.47
6	5.88	3.55	10.62
7	5.12	3.4	19.28
8	4.57	3.25	126.36
9	4.17	3.1	−28.01
10	4.04	2.96	−11.74

Figures 9 and 10 illustrate the effect of Gr/Re on the velocity and temperature profiles, respectively. Buoyancy forces have insignificant effect on the velocity profile in the narrower passage, but for the wider passage significant increase in the velocity near the cooler wall (the baffle in this case) is observed. Gr/Re has less effect on the temperature profile as shown in fig. 10 since the energy equation does not include this parameter.
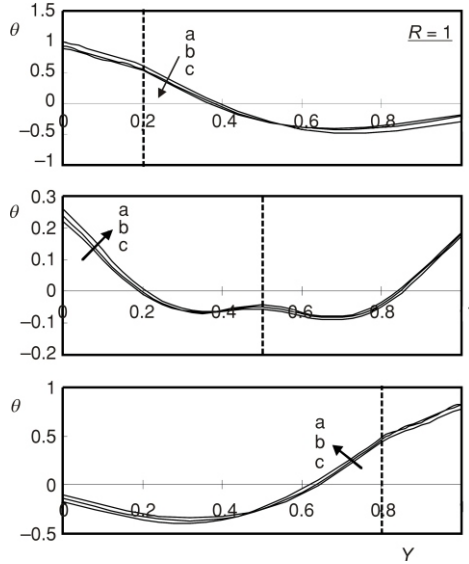
Table 5 presents the variations of Nu$_1$ with Gr/Re at different positions of the baffle for symmetric heating. The table shows that when the baffle is in the middle of the channel, Nu$_1$ is a decreasing function of Gr/Re. Otherwise; Nu$_1$ is an increasing function of Gr/Re. Figure 10 shows that the temperature on wall 1 increases with Gr/Re when the baffle is in the middle of the channel and decreases at the other positions. So, Nu$_1$ changes its trend with Gr/Re as explained before. The effect of Gr/Re on Nu$_1$ for R = 0.5 and 0 is similar to its effect for R = 1.
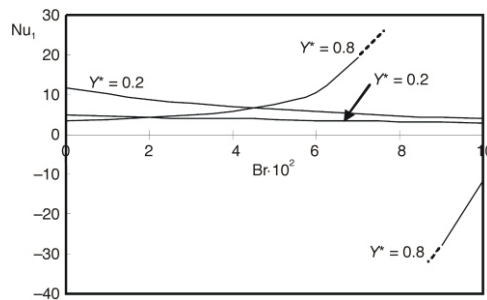
Figure 8. Variations of Nu$_1$ with Br at different positions of the baffle with an adiabatic wall (R = 0.5, Gr/Re = 100)
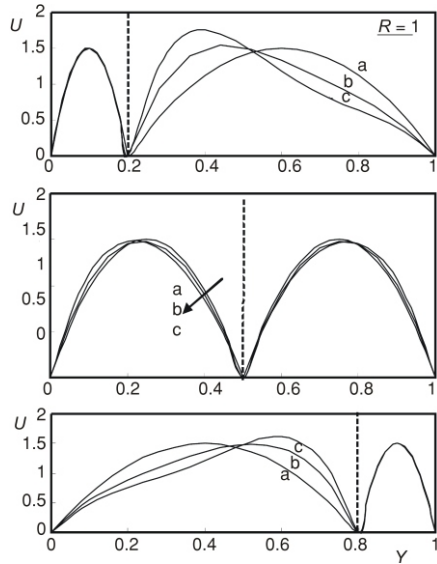
Figure 9. Effect of Gr/Re on velocity profiles for symmetric heating
(a) Gr/Re = 0,(b) Gr/Re = 100, (c) Gr/Re = 200 (Br = 0.05)

Figure 10. Effect of Gr/Re on temperature profiles for symmetric heating
(a) Gr/Re = 0, (b) Gr/Re = 100, (c) Gr/Re = 200 (Br = 0.05)

Table 5. Variations of Nu_1 with Gr/Re at different positions of the baffle for symmetric heating (Br = 0.05)

Gr/Re	$Y^* = 0.2$	Nu_1 $Y^* = 0.5$	$Y^* = 0.8$
0	5.93	4.34	14.83
50	6.2	4.28	16.85
100	6.26	4.2	19.11
150	6.32	4.12	22.4

Conclusions

The effect of viscous dissipation on fully developed laminar mixed convection in a vertical double-passage channel has been studied numerically. Uniform wall heat fluxes with symmetric ($R = 1$), asymmetric ($R = 0.5$), and one wall is adiabatic ($R = 0$) have been considered. The velocity and temperature profiles have been presented and the Nusselt number on the hot wall has been evaluated at different positions of the baffle. It can be concluded that:

– Br and Gr/Re have significant effects on the velocity profiles in the wider passage for all cases. In the narrower passage, these effects are insignificant,
– an increase in Brinkman number leads to a significant increase in the temperature in the narrower passage for all cases. This is accompanied with a significant decrease in the temperature in the wider passage. When the baffle is in the middle of the channel the effect of Brinkman number on the temperature in the whole channel decreases clearly,
– Gr/Re has less effect on the temperature profiles than Br,
– for Y^* 0.5, the Nusselt number on the hot wall is a decreasing function of Brinkman number. When the baffle is far from the hot wall Nu_1 becomes an increasing function of Br. At a certain value of Brinkman number Nu_1 changes its sign. For symmetric heating this change in sign of Nu_1 occurs at less value of Br than for other cases, and
– when the baffle is in the middle of the channel, Nu_1 is a decreasing function of Gr/Re. Otherwise; Nu_1 is an increasing function of Gr/Re.

Nomenclature

b – channel width, [m]
b^* – width of passage 1, [m]
Br – Brinkman number ($= \mu u_0^2/q_1 b$) , [–]
c_p – specific heat at constant pressure, [Jkg^{-1}K^{-1}]
g – gravitational acceleration, [ms^{-2}]
Gr – Grashof number ($= g\beta q b^4/v^2 k$), [–]
h – coefficient of heat transfer, [Wm^{-2}K^{-1}]
k – thermal conductivity, [Wm^{-1}K^{-1}]
n – number of grid points, [–]
Nu – Nusselt number ($= hb/k$), [–]
P – dimensionless pressure ($= p/\rho_0 u_0^2$), [–]
p – pressure, [Pa]
q – heat flux, [Wm^{-2}]
R – heat flux ratio ($= q_2/q_1$), [–]
Re – Reynolds number ($= u_0 b/\ $), [–]
T – temperature, [K]
u – axial velocity, [ms^{-1}]
x – axial coordinate, [m]
y – transverse coordinate, [m]
Y^* – ($= b^*/b$), [–]

Greek symbols

β – volumetric coefficient of thermal expansion, [K^{-1}]
γ – pressure gradient ($= dP/dX$), [–]
θ – dimensionless temperature [$= (T - T_0)/(q_1 b/k)$], [–]
μ – dynamic viscosity, [Pa s]
v – kinematic viscosity, [m^{2}s^{-1}]
ρ – density, [kgm^{-3}]

Subscripts

b   – bulk
0   – reference
1   – value in stream 1
2   – value in stream 2

References

[1] Akbari, H., Borgers, T. R., Free Convective Laminar Flow within the Trombe Wall Channel, *Solar Energy, 22* (1979), 2, pp. 165-174

[2] Hegazy, A. A., Optimization of Flow-Channel Depth for Conventional Flat-Plate Solar Air Heaters, *Renewable Energy, 7* (1996), 1, pp. 15-21

[3] Incropera, F. P., Convection Heat Transfer in Electronic Equipment Cooling, *J. Heat Transfer, 110* (1988), 4, pp. 1097-1111

[4] Teertstra, P., Culham, J. R., Yovanovich, M. M., Lee, S, Analytical Model for the Thermal Behavior of Microelectronic Systems, Advances in Electronic Packaging, ASME, 1995, EEP, Vol. 10, Report 2

[5] Webb, R. L., Principles of Enhanced Heat Transfer, Hemisphere Publ. Comp., Washington, DC, 1995

[6] Candra, P. R., Niland, M. E., Han, J. C., Turbulent Flow Heat Transfer and Friction in a Rectangular Channel with Varying Number of Ribbed Walls, *J. Turbomach., 119* (1997), 2, pp. 374-380

[7] Candra, P. R., Alexander, C. R., Han, J. C., Heat Transfer and Friction Behaviors in Rectangular Channels with Varying Number of Ribbed Walls, *Int. J. Heat Mass Transfer, 46* (2003), 3, pp. 481-495

[8] Han, J. C., Zhang, Y. M., Lee, C. P., Augmented Heat Transfer in Square Channels with Parallel , Crossed and V-Shaped Angled Ribs, *J. Heat Transfer, 113* (1991), 3, pp. 590-596

[9] Lin, Z. H., Chou, Y. J., Hung, Y. H., Heat Transfer Behaviors of a Confined Slot Impingement, *Int. J. Heat Mass Transfer, 40* (1997), 5, pp. 1095-1107

[10] Beitelmal, A. H., Saad, M. A., Patel, C. D., The Effect of Inclination on the Heat Transfer Between a Flat Surface and an Impinging Two-Dimensional Air Jet. *Int. J. Heat Fluid Flow, 21* (2000), 2, pp. 156-163

[11] Dutta, P., Hossain, A., Internal Cooling Augmentation in Rectangular Channel Using Two Inclined Baffles, *Int. J. Heat Fluid Flow, 26* (2005), 2, pp. 223-232

[12] Guo, Z. Y., Li, D. Y., Wang, B. X., A Novel Concept for Convective Heat Transfer Enhancement, *Int. J. Heat Mass Transfer, 41* (1998), 14, pp. 2221-2225

[13] Salah El-Din, M. M., Fully Developed Laminar Convection in a Vertical Double-Passage Channel, *Applied Energy, 47* (1994), 1, pp. 69-75

[14] Salah El-Din, M. M., Developing Laminar Convection in a Vertical Double-Passage Channel, *Heat and Mass Transfer, 38* (2001), 1, pp. 93-96

[15] Salah El-Din, M. M., Effect of Viscous Dissipation on Fully Developed Laminar Mixed Convection in a Vertical Double-Passage Channel, *Int. J. Therm. Sci., 41* (2002), 3, pp. 253-259

[16] Tso, C. P., Mahulikar, S. P., The Use of the Brinkman Number for Single Phase Forced Convective Heat Transfer in Microchannels, *Int. J. Heat Mass Transfer, 41* (1998), 12, pp. 1759-1769

[17] Ho, C. D., Tsai, Y. C., Tu, J. W., Heat Transfer in a Parallel-Plate Channel by Inserting in Parallel Impermeable Sheets for Multi-Pass Coolers or Heaters, *Int. J. Heat Mass Transfer, 47* (2004), 3, pp. 459-476

[18] Aung, W., Fletcher, L. S., Sernas, V., Developing Laminar Free Convection between Vertical Flat Plates with Asymmetric Heating, *Int. J. Heat Mass Transfer, 15* (1972), 11, pp. 2293-2308
[19] Aung, W., Worku, G., Theory of Fully Developed Combined Convection Including Flow Reversal, *J. Heat Transfer, 108* (1986), 2, pp. 485-488
[20] Hamadah, T. T., Wirtz, R. A., Analysis of Laminar Fully Developed Mixed Convection in a Vertical Channel with Opposing Buoyancy, *J. Heat Transfer, 113* (1991), 3, pp. 507-510
[21] Barletta, A., Zanchini, E., On the Choice of the Reference Temperature for Fully Developed Mixed Convection in a Vertical Channel, *Int. J. Heat Mass Transfer, 42* (1999), 16, pp. 3169-3181
[22] Boulama, K., Galanis, N., Analytical Solution for Fully Developed Mixed Convection between Parallel Vertical Plates with Heat and Mass Transfer, *J. Heat Transfer, 126* (2004), 3, pp. 381-388
[23] Aung, W., Worku, G., Developing Flow and Flow Reversal in a Vertical Channel with Asymmetric Wall Temperatures, *J. Heat Transfer, 108* (1986), 2, pp. 299-304
[24] Salah El-Din, M. M., Effect of Thermal and Mass Buoyancy Forces on the Development of Laminar Mixed Convection between Vertical Parallel Plates with Uniform Wall Heat and Mass Fluxes, *Int. J. Thermal Sciences, 42* (2003), 5, pp. 447-453

Author's address:

M. M. Salah El-Din
P. O. Box 2574, Al-Sarai 21411
Alexandria, Egypt

E-mail: msalaheldin 99@yahoo.com